Hindawi Publishing Corporation
Modelling and Simulation in Engineering
Volume 2016, Article ID 5072404, 12 pages
http://dx.doi.org/10.1155/2016/5072404

Research Article

Prediction on Power Produced from Power Turbine as a Waste Heat Recovery Mechanism on Naturally Aspirated Spark Ignition Engine Using Artificial Neural Network

Safarudin Gazali Herawan,[1] Abdul Hakim Rohhaizan,[1] Ahmad Faris Ismail,[2] Shamsul Anuar Shamsudin,[1] Azma Putra,[1] Mohd Tahir Musthafah,[1] and Ardika Ridal Awang[1]

[1]*Centre for Advanced Research on Energy, Faculty of Mechanical Engineering, Universiti Teknikal Malaysia Melaka, Hang Tuah Jaya, 76100 Durian Tunggal, Malacca, Malaysia*
[2]*Department of Mechanical Engineering, Faculty of Engineering, International Islamic University Malaysia (IIUM), P.O. Box 10, 50728 Kuala Lumpur, Malaysia*

Correspondence should be addressed to Safarudin Gazali Herawan; safarudin@utem.edu.my

Received 30 September 2015; Accepted 21 February 2016

Academic Editor: Ahmed Rachid

The waste heat from exhaust gases represents a significant amount of thermal energy, which has conventionally been used for combined heating and power applications. This paper explores the performance of a naturally aspirated spark ignition engine equipped with waste heat recovery mechanism (WHRM) in a sedan car. The amount of heat energy from exhaust is presented and the experimental test results suggest that the concept is thermodynamically feasible and could significantly enhance the system performance depending on the load applied to the engine. However, the existence of WHRM affects the performance of engine by slightly reducing the power. The simulation method is created using an artificial neural network (ANN) which predicts the power produced from the WHRM.

1. Introduction

The number of motor vehicles continues to grow globally and therefore increases reliance on the petroleum and increases the release of carbon dioxide into atmosphere which contributes to global warming. To overcome this trend, new vehicle technologies must be introduced to achieve better fuel economy without increasing harmful emissions. For internal combustion engine (ICE) in most typical gasoline fuelled vehicles, like a typical 2.0 L gasoline engine used in passenger cars, it was estimated that 21% of the fuel energy is wasted through the exhaust at the most common load and speed range [1]. The rest of the fuel energy is lost in the form of waste heat in the coolant, as well as friction and parasitic losses.

Since the electric loads in a vehicle are increasing due to improvements of comfort, driving performance, and power transmission, it is therefore of interest to utilize the wasted energy by developing a heat recovery mechanism of exhaust gas from the internal combustion engine. It has been identified in [2] that the temperature of the exhaust gas varies depending on the engine load and engine speed. The higher the engine load, the higher the temperature of the exhaust gas. Significant amounts of energy that would normally be lost via engine exhausts can thus be recovered into electrical energy. Theoretically, the energy from the exhaust gas can be harnessed to supply an extra power source for vehicles that will result in greater efficiency and also an overall reduction in greenhouse gas emission.

The recent technologies on waste heat recovery of ICE consist of low grade heat from cooling system and high grade heat from exhaust system. For low grade waste heat, the organic Rankine cycle is the favourite choice to recover waste

energy [3], whereas for high grade heat several techniques to recover the energy can be applied such as the thermoelectric generators [4, 5], the turbochargers [6–8], the turbocompounds [9–12], the Rankine cycle system [13, 14], the heat pipe [15], the air conditioning [16], the emission reduction [17], and the power turbine of waste heat recovery mechanism [18]. The approaches lead to theoretical, simulation, or experimental works that may improve the brake specific fuel consumption (BSFC) that means better overall efficiency.

The attractive methods to be explored are turbochargers, and turbocompounds due to the simple construction and low cost. This is because the potential to produce higher output power and the potential to improve BSFC and efficiency are promising. To improve the performance of turbocharger, several studies in [6, 19–21] used electrical motor assisted or integrated starter generator (ISG) for turbocharger or for parallel hybrid power system on a diesel engine [6]. The aim of this method is to improve the fuel economy of diesel homogeneous charge compression ignition (HCCI) that results in increasing in fuel economy, reducing the soot emission, and NO_x emission by 10.9%, 6%, and 12.1%, respectively [6]. The electrical motor assisted turbocharger is the integration of a high-speed 7.5 kW electric motor-generator within a standard turbocharger of a heavy-duty vehicle, where the purpose of this system is to improve the fuel economy and turbo-lag. As a result, this system on an urban bus, the fuel economy can be improved by at least 6% depending on the actual driving cycle. An electrical assist motor can reduce turbo-lag by typically 50% [19–21].

Many studies on the turbocompound are in terms of control strategy [10], parametric geometry [9], dynamic model and characteristic [11, 22], and behaviour of turbocompound based on operating charts for turbocharger component and power turbine [23]. Reference [24] claimed that the application of a turbocompound system is profitable, especially for heavy loaded engines, which can improve power, torque, and fuel consumption by 10-11%, 11%, and 5–11%, respectively.

In control strategy, [10] describes control system developments for an electric turbocompound system on heavy-duty diesel engines. The simulation results done by [10] indicate that at the rated power the fuel consumption of Class 8 on-highway truck engine would be reduced by almost 10%. Considering a typical road load for an on-highway truck, where the engine prevailing operating regime is at 1500 rpm and loads fluctuated between 25% and 50%, overall reduction in fuel consumption is estimated to be around 5% [10]. Reference [9] presents a set of parametric studies of power turbine performed on a turbocompound diesel engine by means of turbine through flow model. By using simulation model, the result is verified and validated with engine performance test data and attained reasonable accuracy. The parametric studies are conducted to analyse the influence of turbine parameters (blade height, blade radius, and nozzle) on engine BSFC, power, expansion ratio, air mass flow rate, and exhaust temperature. As a result, the geometry parameters of turbine (blade height, blade radius, and nozzle exit blade angle) have significant effects on engine BSFC and power [9].

For our concern, there is no application of turbocompound without a turbocharger system in the internal combustion engine. Therefore, this condition is an opportunity to study on the power turbine (turbocompound) at the naturally aspirated spark ignition internal combustion engine that has no turbocharger system, where most studies from literatures are using diesel engines, not a spark ignition engine.

In this study, a simple novel waste heat recovery mechanism (WHRM) is proposed on a passenger car. The WHRM is a device adapted from a turbocharger module, where the compressor part is replaced with a DC generator to produce an output current and voltage. This simple and low cost structure with straightforward energy recovery and with a simple control system is expected to be a great alternative application for an energy recovery system.

Artificial intelligence that has been used in many fields and applications in automotive engineering proved that relationship among different dependent and independent variables or factors could be simulated and modelled to predict or help to make a decision to obtain optimum energy recovery. In this study, artificial neural network (ANN) is selected to do the modelling that simulates the correlation of several variables and factors that affect the output power of waste heat recovery mechanism.

In related internal combustion engine studies, the neural network has been selected for prediction [25–28] and optimization [29]. Reference [30] used neural network for investigating the relative contribution of operational parameters on performance and emission, which is applied on the common-rail diesel engine, while [31] used neural network and incorporated them into conventional mean value models that can present a real-time model with high accuracy and fidelity for spark ignition engine.

ANN is an algorithm that mimics the way human brains do thinking. The more information and trials given through the code produce much better results. This is called training the ANN code. Further reading on ANN can be found in [25–31].

The ANN model has capability to identify, learn correlative pattern, and map even complicated relationships between set of input data and corresponding target values. Compared to the neural network model, traditional prediction models have been developed with a fixed equation based on the limited number of data and parameters. If new data is quite different from original data, then the model would update not only its coefficients but also its equation form. In other words, ANN model does not need such a specific equation form. Once the ANN model is trained, the new input pattern can be put to forecast another output. Instead of that, the neural network model needs enough input-output data. Also, it can continuously retrain the new data set, so that it can adequately adapt to new data.

2. Experimental Setup

The experiment was performed on a Toyota vehicle having 1.6-litre inline four-cylinder gasoline engine. Table 1 shows the specification of the test engine.

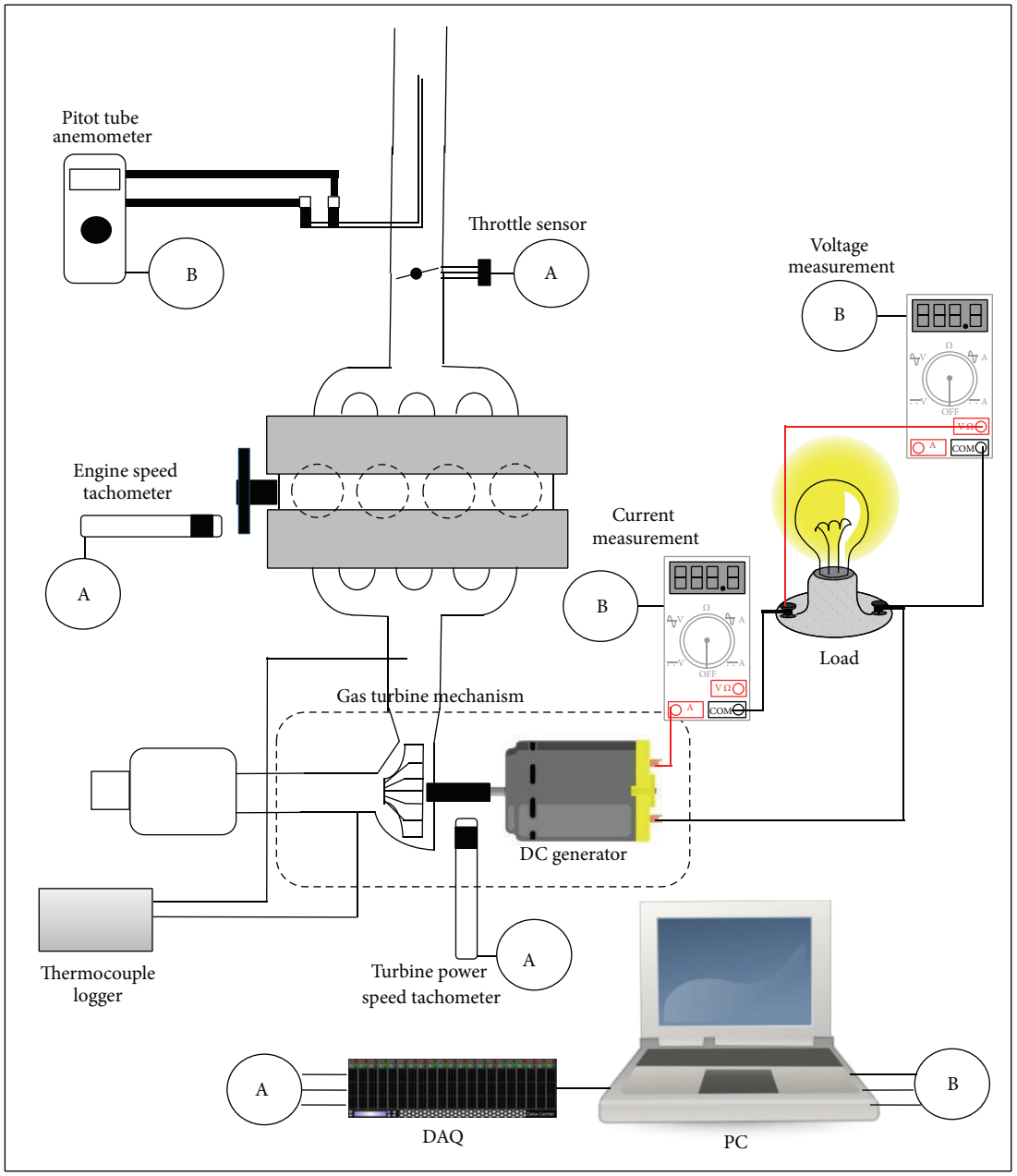

Figure 1: Schematic layout of the experimental setup of waste heat recovery mechanism.

A schematic diagram of the experimental setup is shown in Figure 1. A 75-Watt bulb and 100-Watt bulb were used as a load causing the DC generator to produce an output current and voltage which were recorded in a computer through USB digital multimeter. The air duct to the intake manifold of engine was equipped with a pitot tube digital anemometer to measure the volume flow rate of the intake air. The engine speed and the WHRM turbine speed were continuously monitored using an optical tachometer allowing the digital data to be recorded in a computer through USB data acquisition module. This was also applied for the data of the throttle position for intake air captured using the existing throttle sensor in the experimental vehicle. The test was conducted on the road with variable vehicle speed up to 70 km/h with normal driving and full throttle driving to measure the performance of engine with and without WHRM. Some features of the instrumentation are summarized in Table 2. This study was conducted on the road since there are limited studies doing this method as such [32]. The finding of this study will contribute an important knowledge due to the real load condition, where using the dynamometer is quite difficult for interpreting the real load conditions from the simulated load.

To determine the performance of the engine at full throttle, a simulation program is conducted. This simulation is created in Matlab Simulink environment. The simulation uses

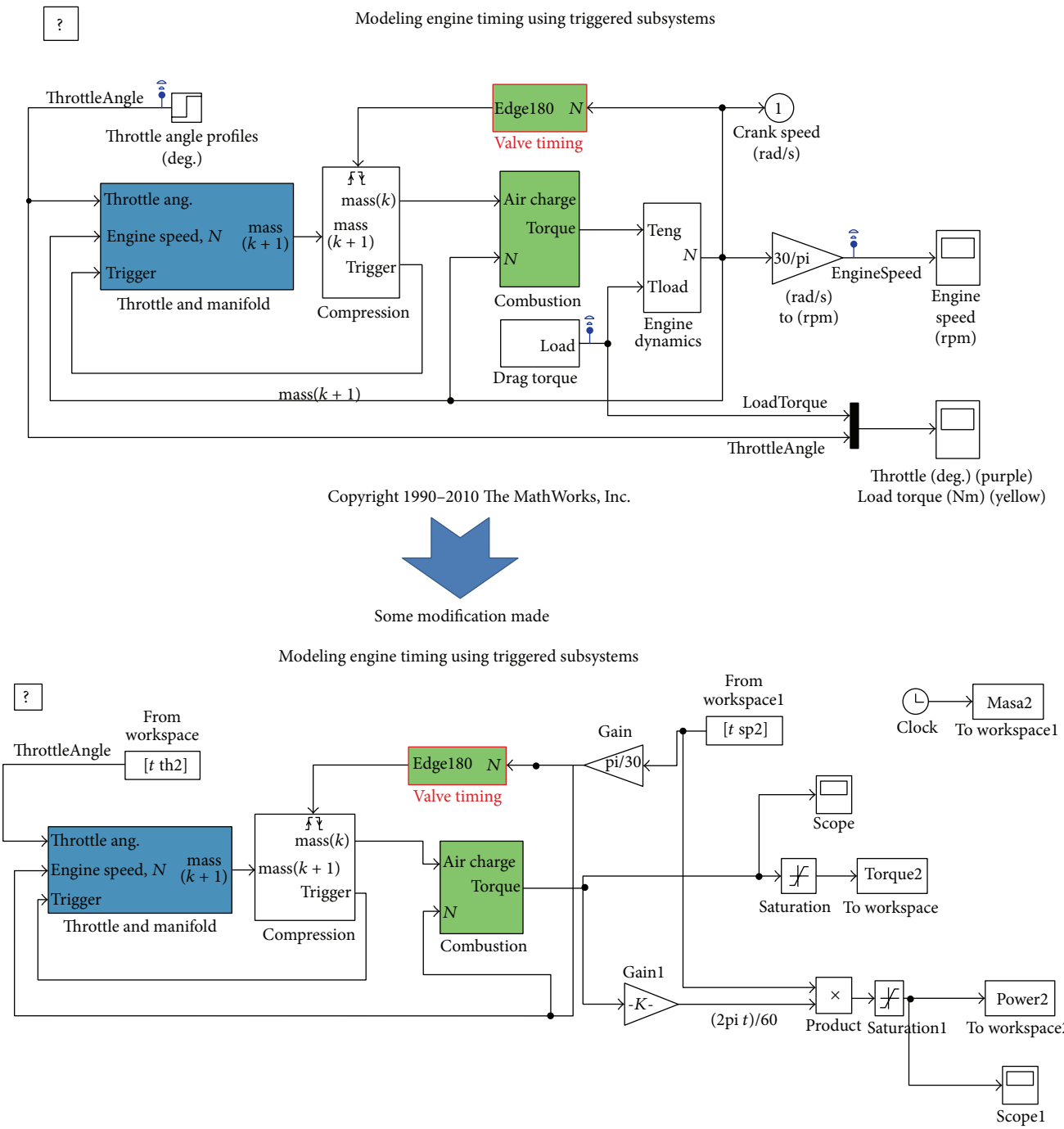

Figure 2: Modified demo Simulink program.

the demo Simulink program [33] with some modification to suit the target. From the simulation, we can get the power and torque of the engine experimental vehicle. The results are needed to compare between before and after implementation of waste heat recovery mechanism, which can then determine whether these mechanisms affect the performance of the engine or not. Figure 2 shows the original demo Simulink program and the modifications made.

3. Results and Discussion

Figures 3, 4, and 5 show the exhaust as a function of engine speed with each time of a second parameter of exhaust temperature, air flow rate, and throttle angle.

The heat energy from exhaust is depending on the engine speed and exhaust temperature; however there are some behaviours not accomplished in this argument. This is because the experimental work was conducted on the

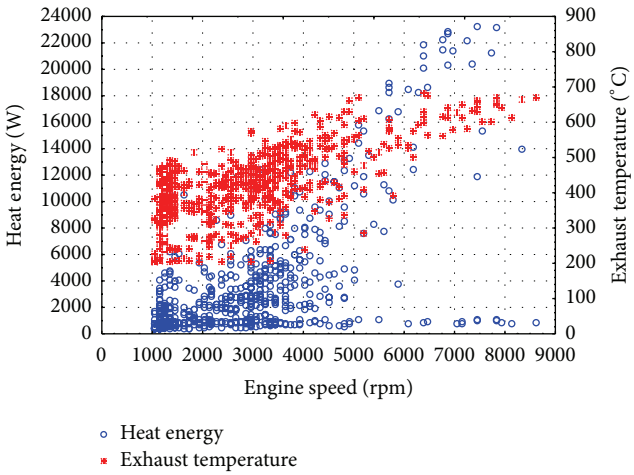

Figure 3: Heat energy from exhaust gas of experimental vehicle on engine speed and exhaust temperature.

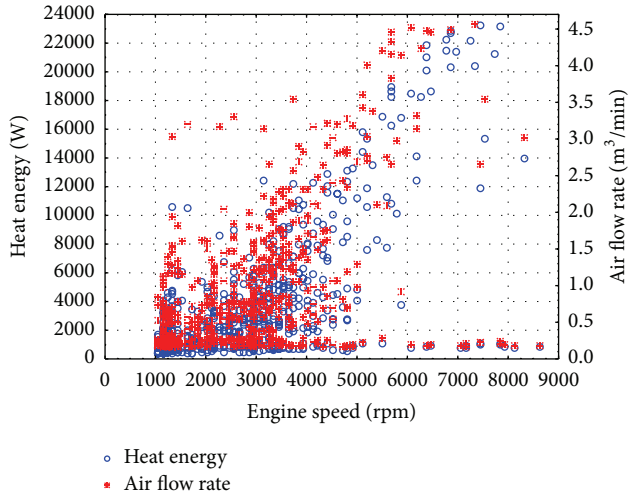

Figure 4: Heat energy from exhaust gas of experimental vehicle on engine speed and air flow rate.

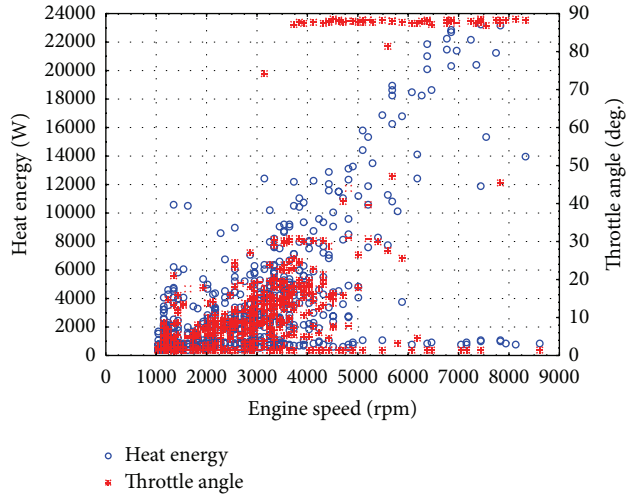

Figure 5: Heat energy from exhaust gas of experimental vehicle on engine speed and throttle angle.

Table 1: Specifications of the test engine.

Type	Specification
Valve train	DOHC 16 valves
Fuel system	Multipoint fuel injection
Displacement	1587 cc (inline)
Compression ratio	9.4 : 1
Bore	81 mm
Stroke	77 mm
Power	112 Hp @ 6600 rpm
Torque	131 Nm @ 4800 rpm

road where no parameter was controlled or fixed. The measurement is based on the normal driving on the road, resulting in the dynamic and transient conditions. The heat energy from exhaust varies in the range of 500 W up to almost 20 kW, which is in good agreement with [34] where the heat energy is in the range of 5 kW and can reach up to 23 kW. Air flow rate gives a significant effect on the heat energy. When the engine speed and exhaust temperature are high, but air flow rate is low, the heat energy follows the air flow rate consistently.

In terms of throttle angle, the increase of throttle angle will increase the heat energy as shown in Figure 5. By applying around 10 to 30 degrees for the normal driving, we can produce 2 kW to 12 kW of heat energy. However, at the full throttle done on the road where the throttle angles are almost 90°, the heat energy value may not be the maximum. This can be attributed to other factors in dynamic and transient conditions. Therefore, to optimize the heat energy from exhaust, we need to increase the throttle angle and load; thus consequently the engine speed, exhaust temperature, and air flow rate will increase. By configurating all of these parameters on the optimum value, the heat energy from exhaust can be generated at the optimum condition. It can be obviously seen that the waste heat energy is high (500 W to 20 kW). Hence, recovering this waste heat energy from exhaust system is worthwhile.

Figure 6 shows the measured data of the parameters which included the normal driving test and full throttle test. Both tests are clearly differentiated by seeing the throttle angle curve, where showing the highest throttle angle achieved (around 87°-88°) was a full throttle test. The full throttle test is tested on the road only for determining the performance of the experimental vehicle in terms of engine power and torque for comparison to vehicle with or without WHRM, not as normal driving.

Also in Figure 6, correlations between all the parameters can be clearly observed; for instance, the air flow rate influences the engine speed, and the higher air flow rate results in a higher engine speed. The change of throttle angle also affects directly the air flow rate, engine speed, and WHRM turbine speed, which eventually changes the output current and voltage accordingly. However, while driving, the load is not known.

In full throttle test, two conditions were applied, which were 2nd- and 3rd-gear positions at the start. It is clearly

Table 2: Details of the instrumentation used in the experiment.

Instrument	Range	Uncertainty
Extech Pitot tube anemometer for air volume flow rate (m^3/min)	0–99,999	±3% rdg.
Existing throttle sensor for throttle angle (degree)	0–90°	—
Compact optical tachometer for engine speed (rpm)	100–60,000 rpm	±0.5%
Compact optical tachometer for power turbine (rpm)	100–60,000 rpm	±0.5%
Pro'sKit USB multimeter for voltage (V)	0–600 V	±(0.5% + 4d)
Pro'sKit USB multimeter for current (A)	0–10 A	±(1.2% + 10d)

rdg. = reading.
d = digits.

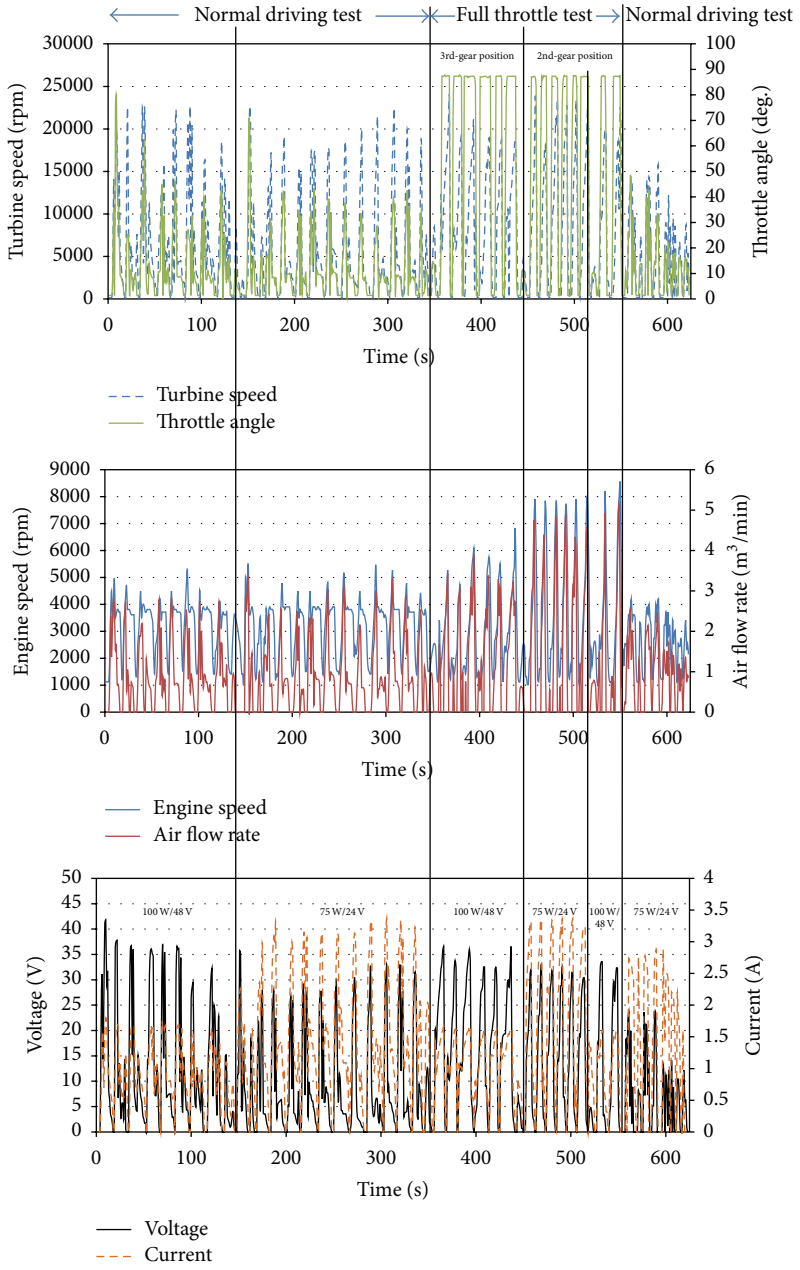

Figure 6: The measured data from the experimental vehicle with WHRM.

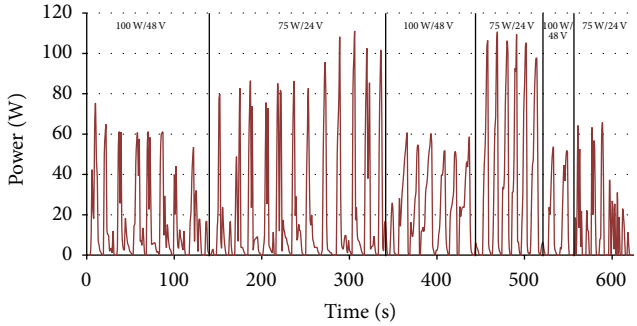

Figure 7: Power generated from WHRM.

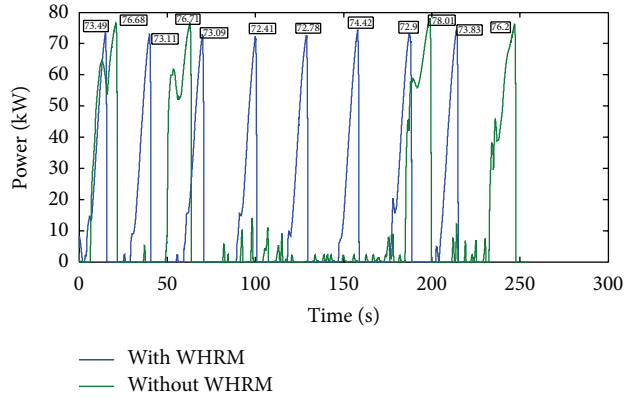

Figure 8: Power of the experimental vehicle with and without WHRM (value in kW).

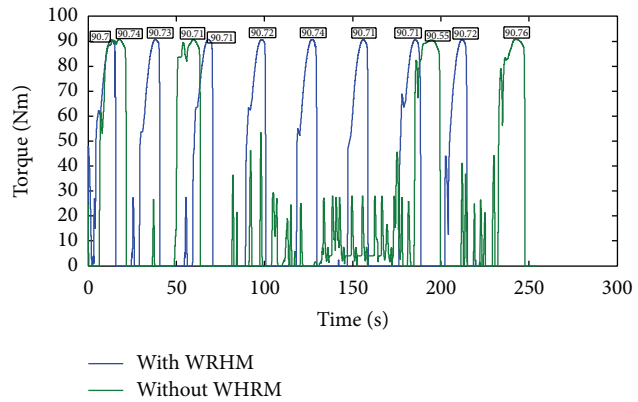

Figure 9: Torque of the experimental vehicle with and without WHRM (value in Nm).

shown that the turbine speed can get higher power value at the 2nd-gear position compared to that at the 3rd-gear condition. At the 2nd-gear position for initial, the engine produces a higher torque to start moving and easily achieved 7000–8000 rpm of engine speed within a few seconds; however in the 3rd-gear condition, the engine would have lower torque causing difficulty in getting engine speed of 7000–8000 rpm in few seconds.

In terms of voltage and current generated by the generator, the higher voltage can be seen at the load of 100 W/48 V as high as 42 volts; however the higher current is at the load of 75 W/24 V as high as 3.3 A. This is due to the torque of the generator. The load of 100 W/48 V generates lower torque for the generator; thus high rpm of turbine can be achieved resulting in higher voltage produced. However, this load has less current to produce due to higher voltage of load. Correlation between torque and current is directly related, where higher current will give a higher torque. Low voltage with higher wattage of load can create a higher current for generator.

Figure 7 shows the power generated from WHRM. It is clearly shown that the load of 75 W/24 V can generate higher power as high as 109 W compared with the load of 100 W/48 V, even though the voltage produced from load of 75 W/24 V is slightly less than the load of 100 W/48 V. Figure 7 also reveals that the performance of WHRM is significantly influenced by the fluctuation of throttle angle, air flow rate, and engine speed during the normal driving and full throttle driving, which results in the power of WHRM being fluctuant. This behaviour also was reported in [34] which explains that it could be difficult to capture a consistent output power of a WHRM. The estimated assembly cost is around Malaysian Ringgit of 2000.00.

Figures 8 and 9 show the power and torque of the experimental vehicle, respectively. It can be seen that the WHRM affects the performance of the experimental vehicle, where the vehicle without WHRM has slightly higher power than the vehicle with WHRM. This is because of the back pressure created from the turbine. The stream of exhaust gas that should be released through the exhaust pipe smoothly was suddenly blocked by the presence of turbine, causing the exhaust system being disturbed. Finally, the power of vehicle becomes slightly decreased from the original power. Another reason is that the experimental vehicle used a naturally aspirated engine, which is not designed to have higher back pressure at the exhaust. The turbocharger engine is more suitable for this circumstance.

The torque of vehicle both with and without WHRM shows a similar value. Therefore the existence of WHRM in the experimental vehicle does not affect much the performance of vehicle in terms of torque.

To predict the power produced from the power turbine, artificial neural network is used to generate mathematical model to determine power produced from several different parameters. Power produced sets as a target and other parameters set as inputs. To select these parameters as inputs, the importance of dependent parameters is needed. Figure 10 shows the importance of parameters to the power produced as a dependent parameter. Here, we can see the strong influence of independent parameter on the dependent parameter by giving a value as F-value. The more the F-value is showed, the higher this independent parameter influences the dependent parameter.

Figure 10 clearly shows that the highest importance parameter is the power turbine speed, followed by throttle angle, air flow rate, and engine speed, respectively. However, power load and voltage load give smallest values of importance to the power produced suggesting these parameters are

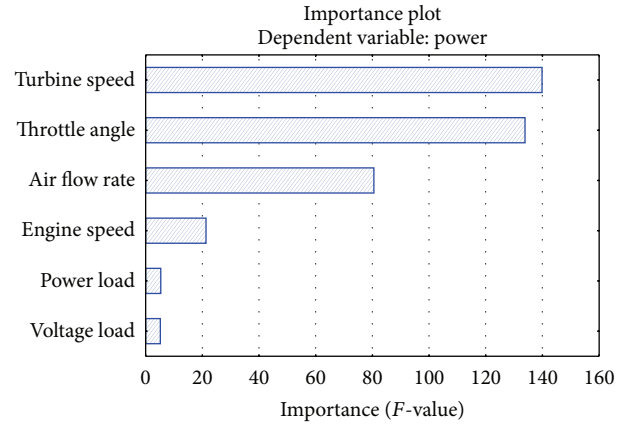

Figure 10: Importance of parameters to power produced as dependent parameter.

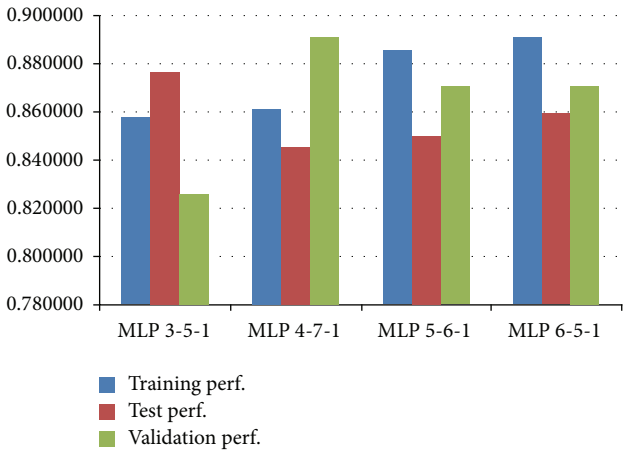

Figure 11: Performance of data training, data test, and data validation in three, four, five, and six input parameters.

not highly relevant to power produced. Based on these results, four simulations of ANN using different input parameters were conducted. The simulation starts from selecting three highest importance values parameters, followed by adding one or more input parameters as needed.

About 70% of data set is used as data training, 15% as data test, and 15% as data validation as suggested by [25–31]. The data test and data validation are data excluded from data training. The introduction of this earlier ANN analysis is conducted using computer software STATISTICA version 6 from StatSoft, Inc. (Dell software). The automated neural network is selected to run the simulation.

Figure 11 shows the performance of data training, data test, and data validation on three, four, five, and six parameters as input parameters. The ANN analysis suggests the network architecture using multilayer perceptrons (MLP), which is a feed-forward neural network architecture with unidirectional full connections between successive layers and applies Broyden-Fletcher-Goldfarb-Shanno (BFGS) algorithm of iterative techniques to train the data.

As shows in Figure 11, the performance of data training is increasing with increasing number of input parameters, similar to data test from four input parameters to higher input parameter. The maximum performance value is 1 when the experimental data is equal to the simulation data. However, the performance of data test at the three input parameters constitutes highest performance. This, however, affects the data validation. Performance of data validation has the highest performance at four input parameters, but it recorded low performance of data training and data validation. Based on the performance in Figure 11, MLP 6-5-1 is being selected as a model to be used for prediction of power produced from power turbine with six input parameters, which are power turbine speed, throttle angle, air flow rate, engine speed, power load, and voltage load.

The correlation between power generated and predicted power generated can be seen in Figure 12. It shows that all data (data training, data test, and data validation) rather accurately scattered near to gradient line (equal to 1) of the prediction model. It means that the ANN can mostly predict the power generated from the six different parameters.

After the ANN analysis, a summary of the network can be seen in Figure 13. The architecture of MLP 6-5-1 of ANN consists of input layer from power turbine speed, engine speed, throttle angle, air flow rate, voltage load, and power load, the 5 neurons of hidden layer, and the output layer of the power produced. Each connection is set to the specific weight and bias.

From the architecture of MLP 6-5-1 in Figure 13, we can generate mathematical model based on input, weight, and bias to determine heat energy. The activation function of each hidden layer is a hyperbolic tangent and the activation function of output layer is an identity. The model is described as follows:

$$P = 0.85246 * h_1 + (-1.17782) * h_2 + 1.80886 * h_3 + 0.69987 * h_4 + 1.77300 * h_5 - 0.24312,$$

$$h_1 = \frac{e^{i_1} - e^{-i_1}}{e^{i_1} + e^{-i_1}},$$

$$h_2 = \frac{e^{i_2} - e^{-i_2}}{e^{i_2} + e^{-i_2}},$$

$$h_3 = \frac{e^{i_3} - e^{-i_3}}{e^{i_3} + e^{-i_3}},$$

$$h_4 = \frac{e^{i_4} - e^{-i_4}}{e^{i_4} + e^{-i_4}},$$

$$h_5 = \frac{e^{i_5} - e^{-i_5}}{e^{i_5} + e^{-i_5}},$$

$$i_1 = (-3.28554) * N_T + 0.23411 * N + 0.85576 * t_\alpha + 1.06459 * V_a + (-1.09712) * V_L + (-1.83310) * P_L - 0.05865,$$

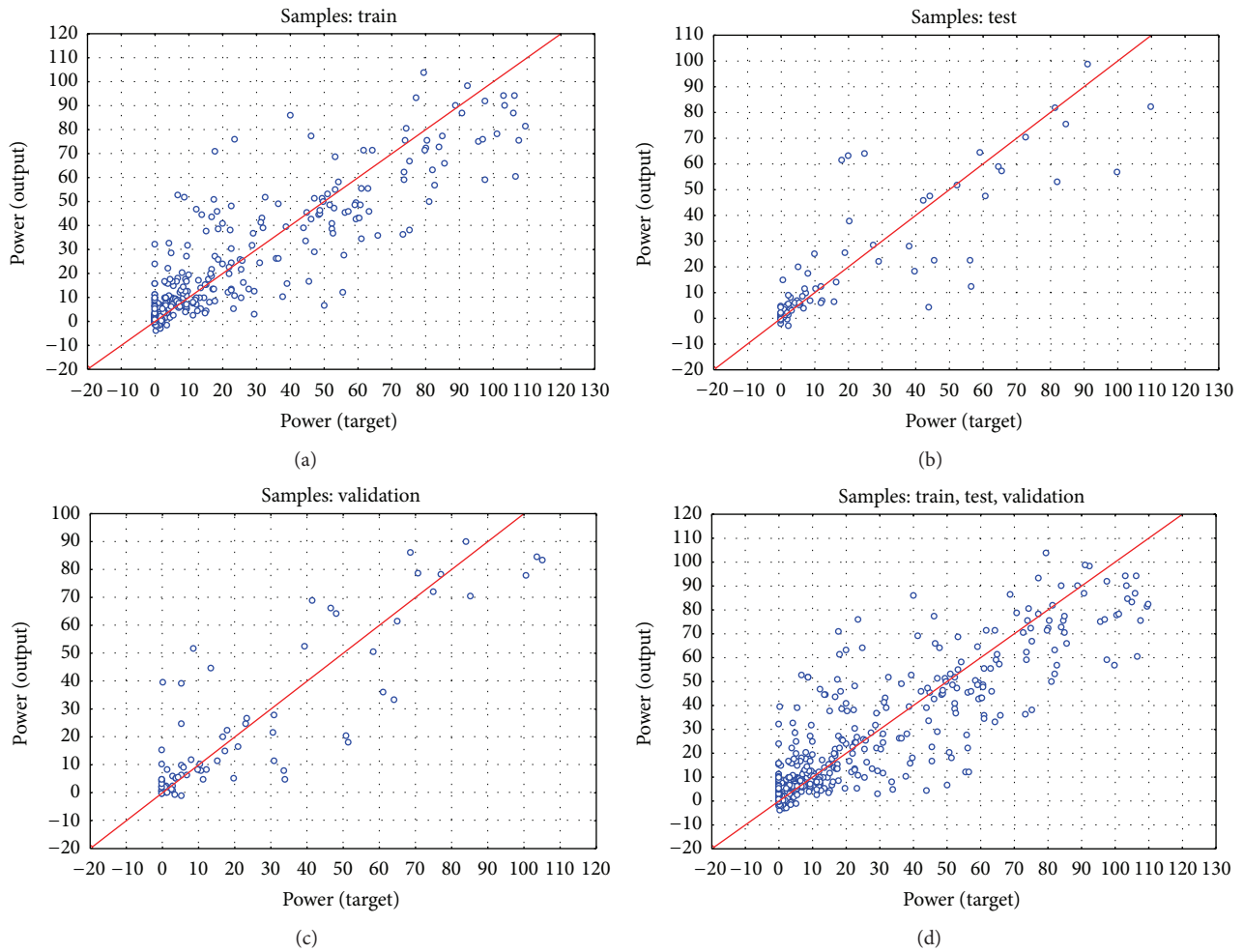

FIGURE 12: The correlation of output of power generated with predicted power generated on data training (a), data test (b), data validation (c), and data overall (d).

$$
\begin{aligned}
i_2 &= 1.16421 * N_T + 0.53723 * N + 0.44149 * t_\alpha \\
&\quad + 0.00868 * V_a + 0.77011 * V_L + 0.46780 \\
&\quad * P_L - 0.90520, \\
i_3 &= 1.21601 * N_T + (-1.61180) * N + 1.78914 * t_\alpha \\
&\quad + (-0.16310) * V_a + 1.03280 * V_L + 0.01030 \\
&\quad * P_L - 0.47420, \\
i_4 &= (-2.26928) * N_T + (-0.05119) * N + 0.08974 \\
&\quad * t_\alpha + (-1.91959) * V_a + 0.31741 * V_L \\
&\quad + 0.09586 * P_L - 0.65251, \\
i_5 &= 0.57925 * N_T + 0.33456 * N + (-0.42188) * t_\alpha \\
&\quad + 0.68826 * V_a + 0.63657 * V_L + (-0.02357) \\
&\quad * P_L + 0.35968.
\end{aligned} \tag{1}
$$

A graph between the experimental power produced and the predicted heat energy is shown in Figures 14 and 15. It can be seen that the ANN simulates the power produced for the entire range of the patterns with good agreement. It means that the ANN analysis can predict power produced that almost 90% of experimental data can be predicted. However, the higher value of power produced could not be tackled by ANN since the results from the experimental vehicle were obtained from a dynamic, nonlinear condition, which might lead to greater uncertainty in the measured results.

Figure 14 shows that the data training is mostly fitted. The simulation can be seen to follow the trend of the experimental data, although disagreement can be observed at some of pattern, where the simulation underestimates the experimental results.

For the data test and data validation sets, comparisons between the experimental results and the ANN prediction for the power produced using 5 hidden neurons are presented in Figure 15. The total of data test and data validation is 30% of total data set. It means 30% of data set of engine speed, throttle angle, air flow rate, voltage load, and power

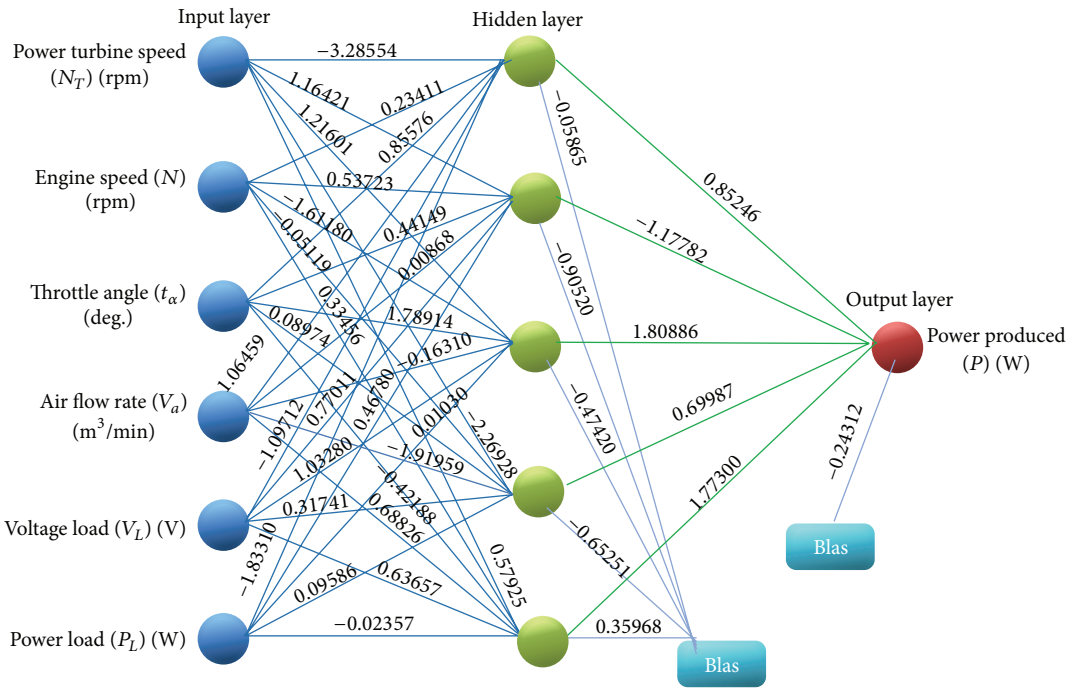

Figure 13: The architecture of MLP 6-5-1 of ANN for prediction of power produced from power turbine speed, engine speed, throttle angle, air flow rate, voltage load, and power load.

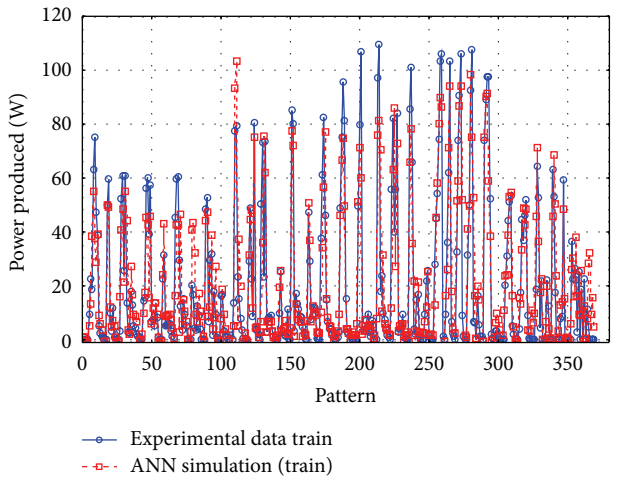

Figure 14: Power produced from experimental results and from prediction ANN analysis on data training.

load as input parameters and power produced as output parameter, not being used for training purposes, can mostly predict the power produced by using the algorithm model generated from ANN analysis, although disagreement also can be observed at some points of the pattern, where the simulation underestimates the experimental results and at some other points overestimates the experimental results, which is similar to the data training sets simulation.

4. Conclusion

Utilization of waste heat energy from the exhaust gas using a WHRM system in a spark ignition engine has been reported. The system has been proven to produce current up to 3.5 A and voltage up to 24 V at normal driving with less traffic. However, the existence of WHRM affects the performance of engine by slightly reducing the power. The ANN prediction model is developed to give reasonably good agreement with the measured data, although few simulation results show disagreement. The proposed system could become a potential energy recovery tool that can be stored in the auxiliary battery to be used for electrical purposes such as air conditioning, power steering, or other electrical/electronic devices in an automotive vehicle.

Competing Interests

The authors declare that there are no competing interests regarding the publication of this paper.

Acknowledgments

The authors would like to acknowledge Universiti Teknikal Malaysia Melaka (UTeM) and the Ministry of Higher Education, Malaysia, for funding support and facilities through the Short-Term Research Project no. PJP/2010/FKM(13B)/S00704 and the Fundamental Research Grant Scheme (FRGS) no. FRGS/2/2014/TK06/FKM/02/F00236.

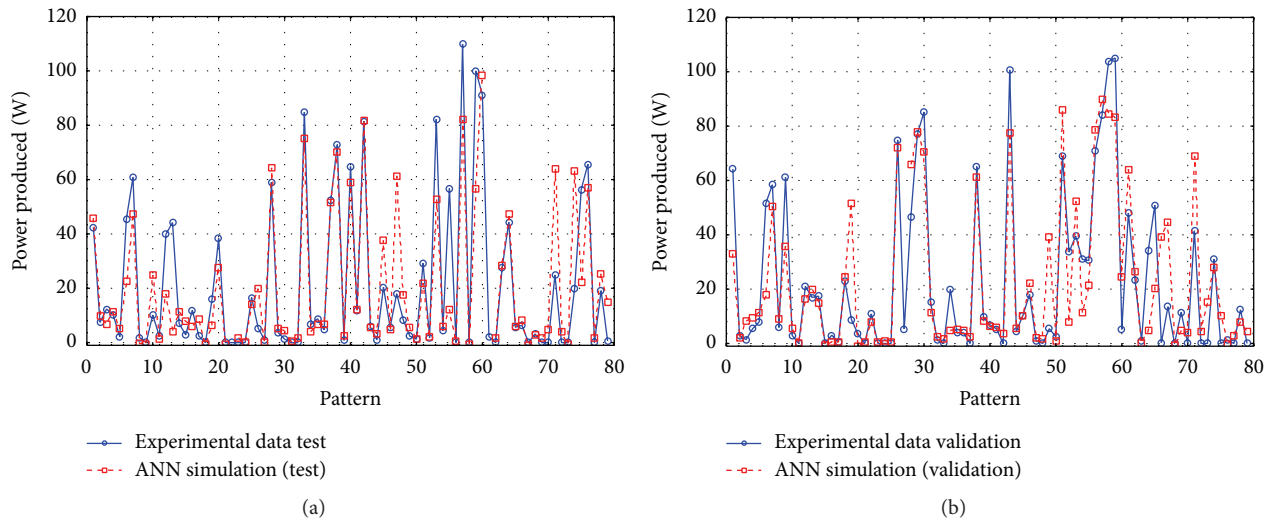

FIGURE 15: Power produced from experimental results and from prediction ANN analysis on data test (a) and data validation (b).

References

[1] R. El Chammas and D. Clodic, "Combined cycle for hybrid vehicles," SAE Technical Paper 2005-01-1171, 2005.

[2] Z. Peng, T. Wang, Y. He, X. Yang, and L. Lu, "Analysis of environmental and economic benefits of integrated Exhaust Energy Recovery (EER) for vehicles," *Applied Energy*, vol. 105, pp. 238–243, 2013.

[3] T.-C. Hung, "Waste heat recovery of organic Rankine cycle using dry fluids," *Energy Conversion and Management*, vol. 42, no. 5, pp. 539–553, 2001.

[4] C. Yu and K. T. Chau, "Thermoelectric automotive waste heat energy recovery using maximum power point tracking," *Energy Conversion and Management*, vol. 50, no. 6, pp. 1506–1512, 2009.

[5] B. Deok In, H. Ik Kim, J. Wook Son, and K. Hyung Lee, "The study of a thermoelectric generator with various thermal conditions of exhaust gas from a diesel engine," *International Journal of Heat and Mass Transfer*, vol. 86, pp. 667–680, 2015.

[6] F. Yang, G. Gao, M. Ouyang, L. Chen, and Y. Yang, "Research on a diesel HCCI engine assisted by an ISG motor," *Applied Energy*, vol. 101, pp. 718–729, 2013.

[7] S. A. Frei, L. Guzzella, C. H. Onder, and C. Nizzola, "Improved dynamic performance of turbocharged SI engine power trains using clutch actuation," *Control Engineering Practice*, vol. 14, no. 4, pp. 363–373, 2006.

[8] M. Tancrez, J. Galindo, C. Guardiola, P. Fajardo, and O. Varnier, "Turbine adapted maps for turbocharger engine matching," *Experimental Thermal and Fluid Science*, vol. 35, no. 1, pp. 146–153, 2011.

[9] R. Zhao, W. Zhuge, Y. Zhang, Y. Yin, Z. Chen, and Z. Li, "Parametric study of power turbine for diesel engine waste heat recovery," *Applied Thermal Engineering*, vol. 67, no. 1-2, pp. 308–319, 2014.

[10] M. Algrain, "Controlling an electric turbo compound system for exhaust gas energy recovery in a diesel engine," in *Proceedings of the IEEE International Conference on Electro Information Technology*, Lincoln, Neb, USA, May 2005.

[11] R. Zhao, W. Zhuge, Y. Zhang, M. Yang, R. Martinez-Botas, and Y. Yin, "Study of two-stage turbine characteristic and its influence on turbo-compound engine performance," *Energy Conversion and Management*, vol. 95, pp. 414–423, 2015.

[12] A. M. I. Mamat, A. Romagnoli, and R. F. Martinez-Botas, "Design and development of a low pressure turbine for turbocompounding applications," *International Journal of Gas Turbine, Propulsion and Power Systems*, vol. 4, no. 3, pp. 1–8, 2012.

[13] Y.-Q. Zhang, Y.-T. Wu, G.-D. Xia et al., "Development and experimental study on organic Rankine cycle system with single-screw expander for waste heat recovery from exhaust of diesel engine," *Energy*, vol. 77, pp. 499–508, 2014.

[14] M. C. Esposito, N. Pompini, A. Gambarotta, V. Chandrasekaran, J. Zhou, and M. Canova, "Nonlinear model predictive control of an organic rankine cycle for exhaust waste heat recovery in automotive engines," *IFAC-PapersOnLine*, vol. 48, no. 15, pp. 411–418, 2015.

[15] F. Yang, X. Yuan, and G. Lin, "Waste heat recovery using heat pipe heat exchanger for heating automobile using exhaust gas," *Applied Thermal Engineering*, vol. 23, no. 3, pp. 367–372, 2003.

[16] W.-D. Wu, H. Zhang, and C.-L. Men, "Performance of a modified zeolite 13X-water adsorptive cooling module powered by exhaust waste heat," *International Journal of Thermal Sciences*, vol. 50, no. 10, pp. 2042–2049, 2011.

[17] F. Will, "Fuel conservation and emission reduction through novel waste heat recovery for internal combustion engines," *Fuel*, vol. 102, pp. 247–255, 2012.

[18] S. G. Herawan, A. H. Rohhaizan, A. Putra, and A. F. Ismail, "Prediction of waste heat energy recovery performance in a naturally aspirated engine using artificial neural network," *ISRN Mechanical Engineering*, vol. 2014, Article ID 240942, 6 pages, 2014.

[19] J. Bumby, S. Crossland, and J. Carter, "Electrically assisted turbochargers: their potential for energy recovery," in *Proceedings of the IET Hybrid Vehicle Conference*, pp. 43–52, The Institution of Engineering and Technology (IET), Coventry, UK, December 2006.

[20] J. Bumby, E. Spooner, and M. Jagiela, "Solid rotor induction machines for use in electrically-assisted turbochargers," in *Proceedings of the 3rd IET International Conference on Power Electronics, Machines and Drives*, Dublin, Ireland, April 2006.

[21] J. R. Bumby, E. S. Spooner, J. Carter et al., "Electrical machines for use in electrcally assisted turbochargers," in *Proceedings of the 2nd International Conference on Power Electronics, Machines and Drives (PEMD '04)*, pp. 344–349, April 2004.

[22] J. Dellachà, L. Damiani, M. Repetto, and A. P. Prato, "Dynamic model for the energetic optimization of turbocompound hybrid powertrains," *Energy Procedia*, vol. 45, pp. 1047–1056, 2014.

[23] C. O. Katsanos, D. T. Hountalas, and T. C. Zannis, "Simulation of a heavy-duty diesel engine with electrical turbocompounding system using operating charts for turbocharger components and power turbine," *Energy Conversion and Management*, vol. 76, pp. 712–724, 2013.

[24] B. Sendyka and J. Soczówka, *Recovery of Exhaust Gases Energy by Means of Turbocompound*, Politechnika Krakowska, Kraków, Poland, 2001.

[25] Y. Cay, "Prediction of a gasoline engine performance with artificial neural network," *Fuel*, vol. 111, pp. 324–331, 2013.

[26] H. Taghavifar, S. Khalilarya, and S. Jafarmadar, "Diesel engine spray characteristics prediction with hybridized artificial neural network optimized by genetic algorithm," *Energy*, vol. 71, pp. 656–664, 2014.

[27] A. Uzun, "Air mass flow estimation of diesel engines using neural network," *Fuel*, vol. 117, pp. 833–838, 2014.

[28] M. Bietresato, A. Calcante, and F. Mazzetto, "A neural network approach for indirectly estimating farm tractors engine performances," *Fuel*, vol. 143, pp. 144–154, 2015.

[29] M. Hooshang, R. Askari Moghadam, S. Alizadeh Nia, and M. T. Masouleh, "Optimization of Stirling engine design parameters using neural networks," *Renewable Energy*, vol. 74, pp. 855–866, 2015.

[30] K. Nikzadfar and A. H. Shamekhi, "Investigating the relative contribution of operational parameters on performance and emissions of a common-rail diesel engine using neural network," *Fuel*, vol. 125, pp. 116–128, 2014.

[31] A.-M. Shamekhi and A. H. Shamekhi, "A new approach in improvement of mean value models for spark ignition engines using neural networks," *Expert Systems with Applications*, vol. 42, no. 12, pp. 5192–5218, 2015.

[32] H. Xie and C. Yang, "Dynamic behavior of Rankine cycle system for waste heat recovery of heavy duty diesel engines under driving cycle," *Applied Energy*, vol. 112, pp. 130–141, 2013.

[33] The MathWorks, *Matlab*, The MathWorks, Natick, Mass, USA, 2009.

[34] N. Yamada and M. N. A. Mohamad, "Efficiency of hydrogen internal combustion engine combined with open steam Rankine cycle recovering water and waste heat," *International Journal of Hydrogen Energy*, vol. 35, no. 3, pp. 1430–1442, 2010.